

## SP-100 THERMOELECTRIC CELL TESTING AT JPL

Richard Ewell and Andrew Zoltan  
Jet Propulsion Laboratory  
California Institute of Technology  
Pasadena, California 91109

### Abstract

Three prototypic SP-100 thermoelectric cells, fabricated by Martin Marietta Astro Space in Valley Forge, Pennsylvania, were tested in vacuum at prototypic temperatures at JPL. Their thermal and electrical performance were characterized with 200°C, 300°C, 400°C, and 500°C temperature gradients across the cell. The latter was representative of prototypic operating conditions with a 1050°C hot side temperature and a 550°C cold side temperature. The initial thermal and electrical performance of all three cells closely matched predictions. Following the characterization testing, the cells were put on an extended life test at the prototypic temperatures, in order to determine any significant degradation modes of the cell. Throughout this test, the thermal performance of the cells were nearly identical to predictions. This test, also, confirmed earlier suspicions that the hot side silicon-germanium to electrode interface would degrade without some significant protective coating at the bond time. Because of resource imitations and early development problems with this coating, the necessary protective layers had not yet been fully developed at the time this generation of cells was manufactured. Subsequent to these tests, accelerated experiments with coupons, having a protective coating applied, have demonstrated the equivalent of 11 to 13 years of operation without any apparent degradation. Four new cells are being fabricated with this technology, two of which will be tested at JPL.

### Test Objective and Purpose

The test program subjected prototypic SP-100 thermoelectric cells to an ingradient thermal vacuum environment. The test objectives were as follows:

1) Verify that the initial electrical and thermal performance of the cell was as predicted and understand any differences between the test data and predicted performance.

2) Validate that the cell degraded with time as predicted, and if there were any differences, determine the probable cause and decide what additional technology developments should be pursued. This was an extension from the original objective for this generation of cells.

### Description of Test Articles

The TA cells were fabricated by Martin Marietta

Astro Space (MMAS), brazed onto hot and cold heat collectors and delivered to JPL for testing. The TA cell configuration is shown schematically in Figure 1 [1-2]. The cell was brazed to a niobium heat collector, on both the hot and cold side, to form the interface with the JPL test fixture. Cell 9 was the first cell fabricated with a porous niobium cold side electrode anti interconnect, previous cells had used porous tungsten.

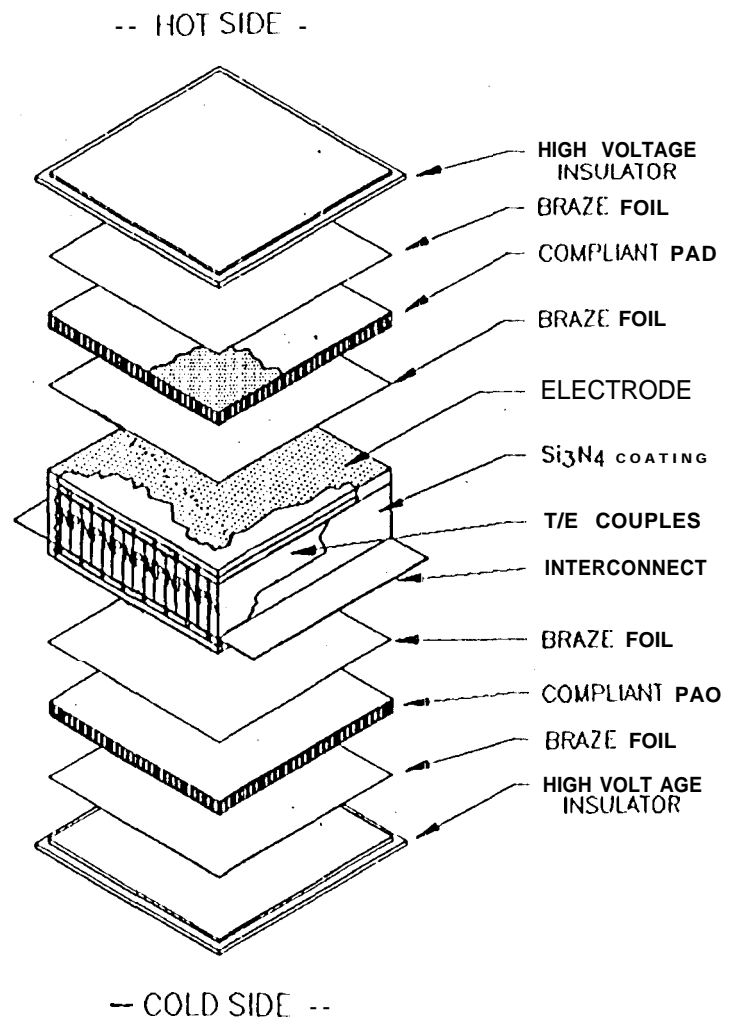


Figure 1. TA cell configuration.

The TA cells consist of the following six components: 1) High voltage insulator, 2) Compliant pad, 3) Low voltage insulator, 4) Electrode, 5) Silicon-germanium (SiGe) multicouple stack, and 6) Heat collectors. The high voltage insulator is required to isolate the series connected cells from ground when they are put into the SP-100 system. Mechanical stresses in

the **thermoelectric cells** were produced by: a) manufacturing, from mismatches in the coefficient of thermal expansion of materials within the cell; b) ingradient operation, from the non-zero coefficient of expansion of the silicon-germanium alloy; and c) ingradient operation, from deflections between the hot and cold heat exchangers. Compliant pads isolated much of the stress from these sources while providing good heat transfer.

The low **voltage** insulator is needed to electrically isolate the electrodes from shorting to the compliant pad. The electrode makes the series connection among the **silicon-germanium** legs within the cell, and provided a means to electrically interconnect the cells on the cold side. The **multicouple** stack consists of alternating legs of n-type and p-type **silicon-germanium** alloy that were bonded together by an insulating glass. There are 8 n-type legs and 8 **p-type** legs.

The hot side heat collector was made of niobium to ensure that no material contamination of the cell could occur and to minimize the mechanical stress put into the cell from thermal expansion mismatches. The heat collector was a simple square plate attached to the hot end of the TA cell with the same braze used in the TA cell fabrication. The other side of the heat collector simply made a metal to metal low pressure contact with the niobium base of the hot side heater. The purpose of the heat collector was to minimize the temperature differential between the TA cell and the heater block. A large area insured that even if the heat transfer was only accomplished by radiation, the temperature drop would still be less than **150°C**. The actual measured temperature differential was about half this, indicating significant conductive heat transfer took place. This low temperature differential was needed to minimize the heater temperature to ensure a long operating lifetime for the heaters. The heat collector was thick enough to be well instrumented with thermocouples, to facilitate the evaluation of the cell thermal performance.

The cold side heat collector was also made of niobium to minimize cell stresses and ensure chemical compatibility. The TA cell was brazed to the cold side heater similarly to the hot side. The cold side heat collector also supported the power leads on either side of the cell. The porous niobium interconnects were bolted to solid niobium bars which were supported on boron nitride blocks that were bolted to the niobium heat collector. The side of the cold heat collector, opposite the cell, mated to the cold side heater.

#### Description of Test Equipment

The test fixture, including the TA cell, was installed above a water cooled copper base plate in a thermal vacuum chamber. The test fixture consisted of a hot side heater, cold side heater, fixture supports, and thermal insulation.

The hot side heater block was fabricated from a niobium bar. The heater block contained four 150 Watt

heaters. Each heater consisted of a molybdenum canister with a molybdenum heating element submerged into the canister. The heating element was insulated from the canister body with high purity alumina powder. The sides of the heater block were wrapped with 16 layers of dimpled molybdenum foil thermal insulation. A **zirconia** block was used to insulate the top side of the heater block. Fiberfrax, fibrous insulation, was placed above the heater to fill the void between the heaters and the **zirconia** insulator.

The cold side heater was fabricated out of a niobium rod. The final shape of the cold side heater resembled a spool. Tantalum wire was coiled around the inner part of the heater block to form the heater element. Alumina beads, that were sectioned off from high purity alumina tubes, electrically insulated the heater wire.

The upper side of the cold side heater interfaced with the niobium cold side heat collector. There was a single layer of gold foil placed between the heater block and the cold side heat collector to enhance the heat transfer between the two bodies. The lower side of the heater was resting on a water cooled copper base plate.

Sixteen type "C" thermocouples were used on the hot side, from the hot heater to and including the hot junction. Sixteen type "E" (**chromel-constantan**) thermocouples were used on the cold side. These were used from the cold junction down to the cold side heater, **Six voltage** taps were attached to the cell.

The test and control rack consisted of the following components: alarm panel, DVM function panel, temperature function panel, load and load control panel, and the hot and cold side heater panels. The alarm panel was used to monitor and control system failure modes. Upon the detection of a loss of water coolant, loss of vacuum (pressure in excess of  $8 \times 10^{-4}$  torr), or major power interruption the system would interrupt the cell operation and shut down both the hot and cold side heaters to protect the thermoelectric cell from being damaged. In addition, both the hot and cold side heat collector temperatures were monitored and if either exceeded a set limit (1300°C at the hot side or 800°C at the cold side), the cell operation would be interrupted by shutting down the hot and cold side heaters.

The load and load control panel enabled the adjustment of the cell output power from short circuit mode (**Isc**) to open circuit mode (**Eoc**). An open-circuit trigger circuit was installed to temporarily break the circuit to allow for measurement of the open circuit voltage. The load controller allowed for the performance of parametric tests and the determination of the cell maximum power output. The load was controlled by a power supply in series with the cell and a shunt resistor. The shunt resistor was used to monitor the cell current.

The vacuum chamber was composed of a water cooled stainless steel bell jar, a cryogenic high vacuum pump and controller. The controller was connected to the alarm panel to provide for the safe operation of the cell. A vacuum of better than  $5 \times 10^{-6}$  torr was maintained throughout the test,

## Test Procedure

Upon receipt of the TA cell from MMAS a visual inspection was performed and the location of any visible cracks on the exterior of the cell were noted. Color photographs were taken of the cell to document its status. The room temperature cell resistance was measured and a voltage map was made of the cell. All of the requisite thermocouples and voltage taps were attached to the cell, the cell was put into the test fixture, and the test fixture was put into the vacuum chamber.

The vacuum chamber was sealed and pumped down until a vacuum of less than  $5 \times 10^{-5}$  torr was obtained. Power was applied to both the hot and cold side heaters to heat the cell isothermally up to a uniform temperature of  $550^{\circ}\text{C}$ . At this point the cell resistance was measured. Then the power to the hot side heater was increased and the power to the cold side heater was reduced until a stable operating condition with a  $200^{\circ}\text{C}$  temperature differential across the cell was obtained. The cold side cell temperature was  $550^{\circ}\text{C}$  and the hot side cell temperature was  $750^{\circ}\text{C}$ . Once the cell was stabilized at this operating condition, steady-state data was taken for a minimum of 5 "different load resistances. This was repeated with a  $300^{\circ}\text{C}$ ,  $400^{\circ}\text{C}$ , and  $500^{\circ}\text{C}$  cell temperature differential. Following cell characterization the cell was put on extended test with a prototypic  $500^{\circ}\text{C}$  cell temperature differential.

## Cell Performance Characterization Test Data

Although three cells were tested at JPL, test data and analysis will only be presented for the first cell tested, TA Cell 9. This test data is representative of the other two cells.

The first test done on the cell, following the initial verification of the test facility, was a parametric study of the electrical and thermal characteristics of the cell. The cell was tested at a minimum of five different load points with four different nominal temperature differentials across it. This first set of tests was done to determine the cell initial performance and find out how the cell performance compared to predictions.

During the initial characterization of the cell, comparisons were made between the predicted temperature profile and the actual thermocouple measurements. Figure 2 shows a comparison made at one of the  $500^{\circ}\text{C}$  data points for TA Cell 9. The figure shows that there is an excellent match between the thermocouple measurements and the predicted temperature profile. The predicted profile was based on the input of a load resistance that gave a perfect match to the measured current. Hot and cold side fixture temperatures that closely matched those measured for the cell and give an exact match between the predicted open circuit voltage and the measured open circuit voltage were chosen. The predicted temperature profile matches the thermocouple measurements within the accuracy capability of the thermocouples. The only exception to this is within the silicon-germanium legs

themselves and this is because the figure indicates a linear temperature gradient between the hot and cold junction temperatures and this is not realistic. As a result of Peltier cooling at the hot junction and Peltier heating at the cold junction the actual profile will be non-linear. The actual temperature near the hot side thermocouple location should be below the prediction line and those near the cold junction should be above the prediction line. In both cases the thermocouple readings follow this trend.

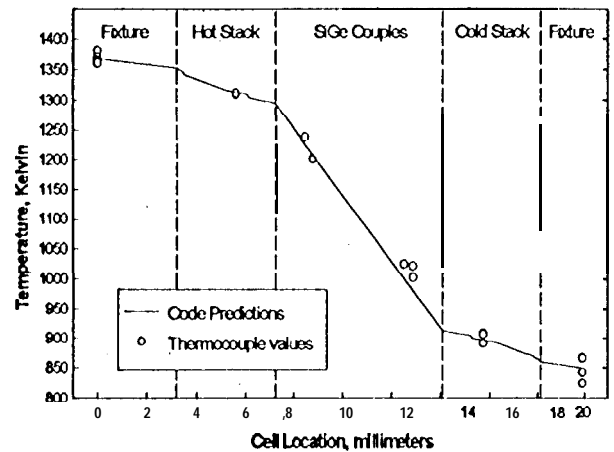


Figure 2. Initial Temperature Profile Comparison

During the initial characterization of the cell, comparisons were made between the predicted electrical performance of the cell and the actual measured current and voltage output of the cell. Figure 3 shows a comparison of the  $500^{\circ}\text{C}$  data points and the predicted I-V cell characteristics. There is a reasonable match, however, as indicated by the slope of the I-V curve, the actual cell has a slightly higher internal resistance than was predicted. This is apparently the result of higher than predicted electrical contact resistances between the SiGe

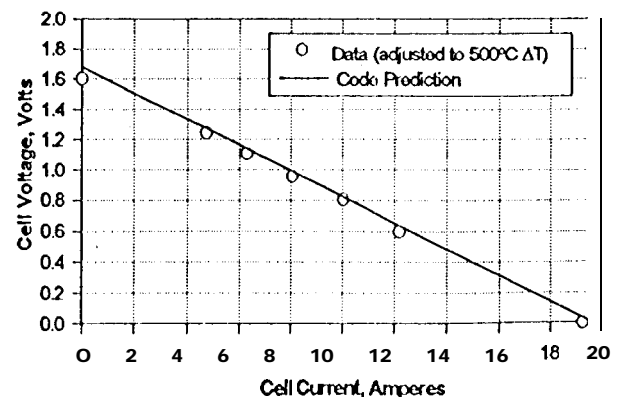


Figure 3. Initial TA Cell 9 I-V Curve Comparison at  $500^{\circ}\text{C}$

and the graphite of the electrode. Figure 4 shows a comparison of the 500°C data points and the predicted cell power output as a function of current. There is again a reasonable match, however, the measured peak power is slightly less than predicted and the power at high currents is lower than predicted. Similarly, this is the result of the higher than predicted cell internal resistance.

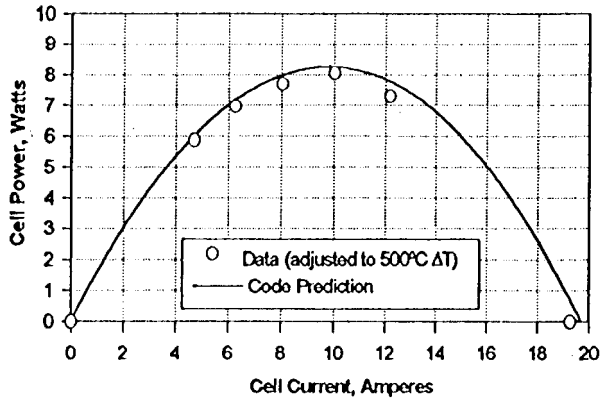


Figure 4. Initial TA Cell 9 I-P Curve Comparison at 500°C

#### Extended Life Test

Following the completion of the cell performance characterization under prototypic conditions, the cell was put on an extended life test with a fixed load at these same prototypic conditions. The extended life test was done to learn how the cell degrades with time, and to compare this degradation to predictions. The extended life test was not an initial objective for this class of cells but, was done as an additional objective. This test was done to confirm earlier suspicions that the hot side electrode bond would degrade without some significant protective coating at the bond line.

The cell accumulated a total of 488 hours of time on test with the hot side temperature above 700°C because of the cell characterization tests, before it was put on extended life test. It remained on test for an additional 1800 hours, at which time the cell was taken off test and a destructive examination done.

The main deviation between the predicted cell performance and the actual cell performance over time was a result of a rapid increase in cell internal resistance. This is shown in Figure 5 which shows the measured cell internal resistance as a function of time at temperature against the predicted increase that would result from dopant precipitation. The curve shows that the internal resistance increased by nearly a factor of three over the 2800 hours of time on test. This compares to an expected increase of only 20% over this time period. This increase in cell internal resistance was the result of deterioration of the hot side SiGe to graphite interface. This interface deteriorated so significantly that there was an actual separation between the outermost n-leg and the

graphite on the hot side, as noted during the post test examination.

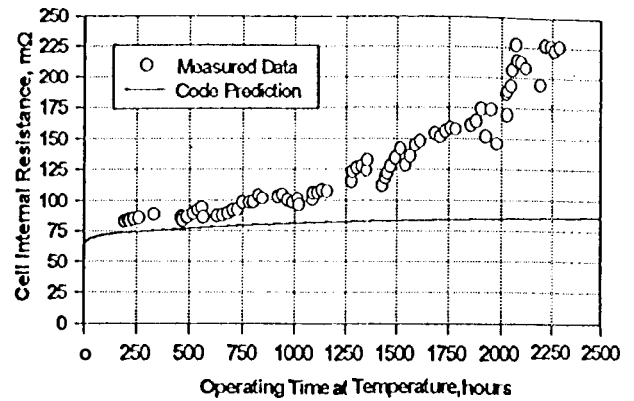


Figure 5. TA Cell 9 Resistance Degradation Comparison

Figure 6 shows the temperature corrected cell peak power output as a function of time. Two corrections were made: one to adjust the cell power to represent the power at the peak power voltage, and second to correct the power for temperature deviations away from the nominal 500°C operating point. The adjustment for the peak power is made by taking peak power to be:  $Power = E_{oc}^2 / (4 * R_{in})$ . This adjustment is reasonable if the cell is operating near the peak power current, so that the temperature would not change much in going to the peak power point. The temperature correction is:  $P_{500} = (500 / Cell \Delta T)^2 * Power$ . The plot shows that the cell power decreases considerably more than predicted. Again this is a result of the increased cell internal resistance.

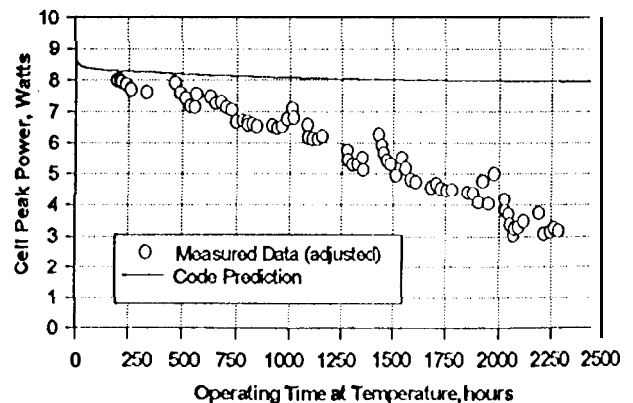


Figure 6. TA Cell 9 Power Degradation Comparison

Figure 7 shows how the cell thermal performance varies with time. It shows the deviation between the measured open circuit voltage against the predicted open circuit voltage. The prediction is based on using the measured fixture temperature and measured current as inputs to the code and using the assumed time dependence of the SiGe Seebeck coefficient. The figure

indicates that there is excellent agreement between the two. This shows that the thermal performance remained good throughout the duration of the test.

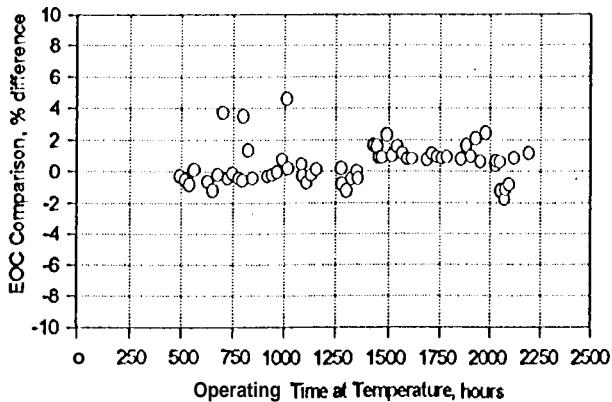


Figure 7. TA Cell 9 Open Circuit Voltage Comparison

#### Post Test Evaluation

After the TA Cell 9 was taken off test at JPL, the cell was examined under an optical microscope and the cell resistance was mapped. Under an optical microscope it was evident that there was nearly a complete debond at the outermost n-type SiGe to graphite interface at the hot end on one side of the cell. No significant crack was observed on the other side, and it was not possible to see along the end to determine the extent of the crack.

Further evidence for the deterioration of TA Cell 9 comes from a comparison of the room temperature voltage maps taken at the beginning of testing and at the end of testing. By examining the initial voltage map it is apparent that the contact resistance between the SiGe and the graphite electrodes is approximately the same throughout the cell. Whereas, by examining the voltage map at the end of testing, it is apparent that the hot side bond resistances have changed significantly, but the cold side bond resistances are very similar to the beginning of test values. The outermost hot side n-type SiGe/graphite bond resistance had gone up about 240 times over its initial value. The adjacent n-type SiGe/graphite bond resistance had increased by about 15 times over its initial value. The four central n-type SiGe/graphite bonds had their resistance increased by about 4 to 5 times their initial value. The resistance of the n-type SiGe/graphite bond for the couple with the outermost p-leg had a resistance increase of about 35 times. The resistance of the adjacent n-type SiGe/graphite bond had increased by about 13 times. This shows that the n-type SiGe/graphite bond deteriorates with time at temperature and that the outermost bonds are most affected. A similar deterioration occurred with the p-type SiGe/graphite bond, but to a much lesser extent. The bond where the p-leg was outermost, had about a 20 fold increase in contact

resistance as a result of time at temperature. The p-type SiGe/graphite bond, of the couple where the n-leg was outermost, had about a 2 times increase in electrical contact resistance. The six innermost p-type SiGe/graphite bond resistances were not significantly affected.

#### Conclusions

The initial thermal and electrical performance of three prototypic SP-100 thermoelectric cells tested was excellent. Their thermal performance was nearly identical to predictions. This shows that even with the large number of different layers that make up the SP-100 thermoelectric cell, excellent thermal performance is possible. This excellent thermal performance was maintained throughout the entire test period. The initial cell electrical performance, also, closely matched predictions. All three cells produced nearly 8 Watts of electrical power under prototypic conditions.

Following characterization testing, the cells were put on an extended life test at prototypic temperatures, in order to determine any significant degradation modes of the cell. Throughout this test, the thermal performance of the cells were nearly identical to predictions. This test confirmed earlier suspicions that the hot side silicon-germanium to electrode interface would degrade without some significant protective coating at the bond line. Because of resource limitations and early development problems with this coating, the necessary protective layers had not yet been fully developed at the time this generation of cells was manufactured. Subsequent to these tests, accelerated experiments with coupons, having a protective coating applied, have demonstrated the equivalent of 11 to 13 years of operation without any apparent degradation. Four new cells are being fabricated with this technology, two of which will be tested at JPL.

#### Acknowledgement

The research described in this paper was carried out by the Jet Propulsion Laboratory, California Institute of Technology, under contracts with the National Aeronautics and Space Administration and the Department of Energy.

#### References

1. J. Bond, D. Matteo, & R. Rosko, "Evolution of the SP-100 Conductively Coupled Thermoelectric Cell", Proceedings of the Tenth Symposium on Space Nuclear Power and Propulsion; Albuquerque, NM, 1993.
2. C. England & R. Ewell, "Progress on the SP-100 Power Conversion Subsystem", Proceedings of the Eleventh Symposium on Space Nuclear Power and Propulsion; Albuquerque, NM, 1994.